P12.2

ENVIRONMENTAL ANALYSIS AND PHOTOGRAPHIC DOCUMENTATION OF AN INTENSE, LEFT-MOVING SUPERCELL ON THE COLORADO PLAINS

Roger Edwards[1]
Storm Prediction Center, Norman, OK

Stephen J. Hodanish
National Weather Service Forecast Office, Pueblo, CO

1. INTRODUCTION AND BACKGROUND

Supercells moving leftward of the mean wind vector, in the northern hemisphere, characteristically contain a mesoanticyclone (after Davies-Jones 1986) which typically is treated as the conceptual mirror image of its right-moving counterpart. Left-moving supercells often produce damaging wind, and may rarely spawn tornadoes (i.e., Monteverdi et al. 2001, Dostalek et al. 2004, Edwards et al. 2004). The dominant threat with anticyclonic supercells, however, is large hail. They often produce significant (≥2 inch or >5 cm) hail, particularly in environments characterized by large vertical shear and buoyancy which also support extremely large, damaging hail from right moving supercells (i.e., Mathews and Turnage 2000, Edwards et al. 2004).

Many left-movers are observationally documented (i.e., Nielsen-Gammon and Read 1995) to have developed from the storm-splitting process similar to those ideally depicted in numerical models (i.e., Klemp and Wilhelmson 1978, Weisman and Klemp 1982). Some, however, form discretely and deviate to the left of the mean shear soon after genesis.

Here we examine an anomalously intense, anticyclonic supercell affecting a relatively remote area around Aroya, in Lincoln and Cheyenne Counties, Colorado, on the afternoon of 15 June 2002. The supercell produced hail up to 5 cm (2 inches) in diameter, accumulating up to 10 cm (4 inches) deep. This storm is documented and analyzed using multiple observational platforms, including satellite imagery, radar imagery and field photography. The storm's evolution and morphology is examined and compared across both remotely sensed and directly observed perspectives – a common theme for observational studies of cyclonic supercells but not for left-movers.

We illustrate a persistent and anomalously intense mesoanticyclone in this storm during the period of its most leftward deviant motion. Observational data

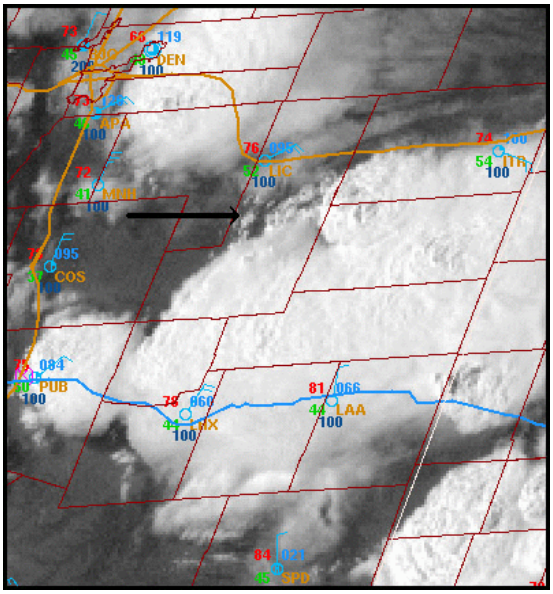

Figure 1. GOES visible satellite image over eastern Colorado, 2232 UTC, 15 June 2002, with county borders, conventional surface plot and Interstate highway routes overlaid. Arrow indicates convective tower associated with genesis of left-moving supercell.

---

and RUC model soundings (Thompson et al. 2003) are used to evaluate the near-storm environment and assess the predictability of its unusual, east-southeastward average motion for a left-moving supercell. The environment – both in storm-relative and Galilean-invariant frameworks – changed rapidly before storm initiation from one favoring right-moving supercells to one favoring left-movers. We illustrate the associated adjustments in vertical shear and buoyancy related to the passage of a cold front prior to the storm's genesis. Finally, ground photography of the storm at peak intensity is presented, inverted into mirror image and compared to similar imagery of cyclonic supercells, for utility in both conceptual relation and in visual recognition by storm spotters.

[1]Corresponding author address: Roger Edwards, Storm Prediction Center, Norman, OK
e-mail: Roger.Edwards@NOAA.gov

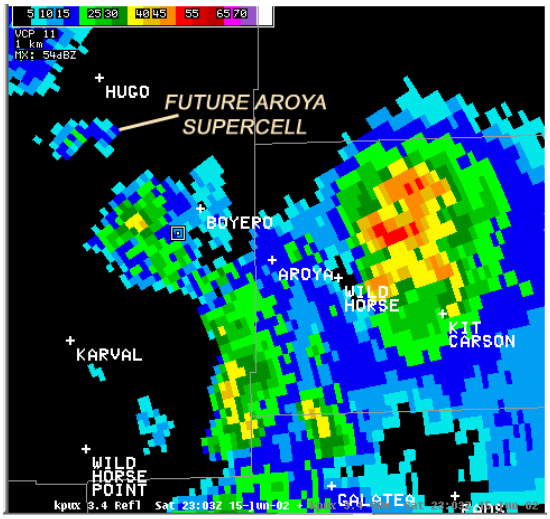

Figure 2. Reflectivity image at 3.4^{O} elevation from Pueblo, CO WSR-88D, 2303 UTC, 15 June 2002, denoting the initial echo of the Aroya storm. The 0.5^{O} echo centroid appeared at 2308 (Fig. 3) and was displaced slightly farther south due to tilting of the convective column. Values are scaled at top and range from 5 to ~55 dBZ in the echo.

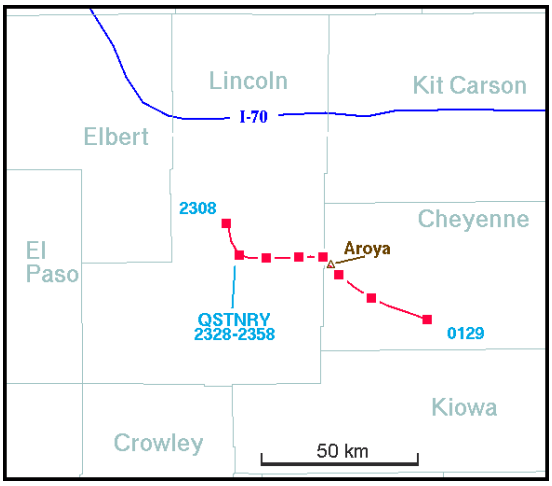

Figure 3. Track of 0.5^{O} reflectivity centroid for the Aroya supercell over eastern Colorado. Times are labeled in UTC. Unlabeled points are every three volume scans (~15 min) apart. Nearby counties, Aroya and Interstate 70 are designated.

---

2. DOCUMENTATION AND MORPHOLOGY

For brevity, all times are given in UTC hereafter unless otherwise noted. The Aroya storm developed discretely, and not as a result of any storm splitting processes. The first convective towers associated with this cell were evident on visible satellite imagery (Fig. 1) over west-central Lincoln County at about 2230, with initial reflectivity appearing aloft around 2303 (Fig. 2) on the 3.4^{O} tilts from the WSR-88D radar at Pueblo, CO (PUX). This storm then followed a winding, 50 mi (80 km) long, roughly east-southeastward track. The path consisted of four sharply defined motion stages, for approximately 2.5 h across Lincoln and Cheyenne Counties before dissipating (Fig. 3).

The echo initially moved southeast (from 335^{O}) at 18 kt (9 m s^{-1}), slower than and slightly to the right of the southeastward mean wind vector (from 305^{O} at 25 kt or 12 ms^{-1}). The nascent supercell became nearly stationary for about 0.5 h beginning 2328 UTC. During this phase it interacted with and nearly was absorbed into a previously stronger thunderstorm to the southeast (WSW of Boyero in Fig. 2). The two storms' reflectivity patterns merged to the extent that at 2348 their cores – though still discretely recognizable – were separate only at reflectivities $\geq$ 50 dBZ. The southern storm's core weakened as the Aroya storm began to move again. The former accelerated and turned sharply to the left, moving eastward (from 270^{O}) at 20 kt (10 m s^{-1}) toward both the Cheyenne County line and the nearby crossroads representing the former town of Aroya. Meanwhile, the southern storm became better separated until the latter's dissipation at roughly 0045 16 Jun.

During the mature phase of most deviant leftward motion, the Aroya storm developed a pronounced, northward-tilting, front-flank reflectivity overhang (Fig. 4) and a mesoanticyclone. These formed mirror images of two characteristics associated for decades with mature cyclonic supercells (i.e., Lemon and Doswell 1979). The mesoanticyclone persisted for uncommon strength for a left-mover. Initial anticyclonic shear became apparent in storm-relative motion (SRM) data at 0014 on 16 June, at 0.5^{O} elevation from PUX.

The storm's anticyclonic vortex remained most strongly evident at the 0.5^{O} tilt angle, from both PUX and Goodland, KS (GLD) radars. The associated shear couplet weakened with height but extended to between 2.4^{O} and 3.4^{O} elevation, as sensed by each radar. [Throughout much of this interval of greatest leftward deviance, some portions of the storm were mired intermittently in range-folded data voids and/or dealiasing errors at the lowest elevation from PUX and/or GLD; so mesoanticyclonic continuity is inferred from a blend of all available elevation segments of each site's SRM depictions.]

The mesoanticyclone deepened vertically and strengthened until reaching a peak azimuthal shear intensity of at least 100 kt (50 m s^{-1}) from PUX at 0034 (Fig. 5a), representing roughly 50 kt (25 m s^{-1}) outbound *and* inbound SRM values across adjacent gates at the resolution of the display. A similarly intense but more convergent anticyclonic signature was evident simultaneously from GLD (Fig. 5b). 80-

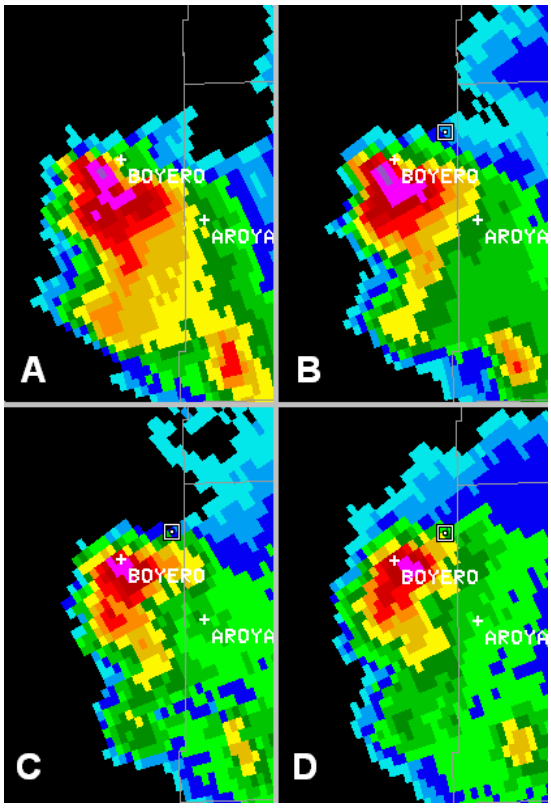

Figure 4. Pueblo CO radar reflectivity images from a) 0.5°, b) 1.5°, c) 2.4°, and d) 3.4° elevation angles, following intensity and mapping conventions of Fig. 2. Spatial scale is identical for each panel. The top of the letter "B" in Boyero represents an effective marker for the horizontal extent of the 30-75 dBZ reflectivity overhang.

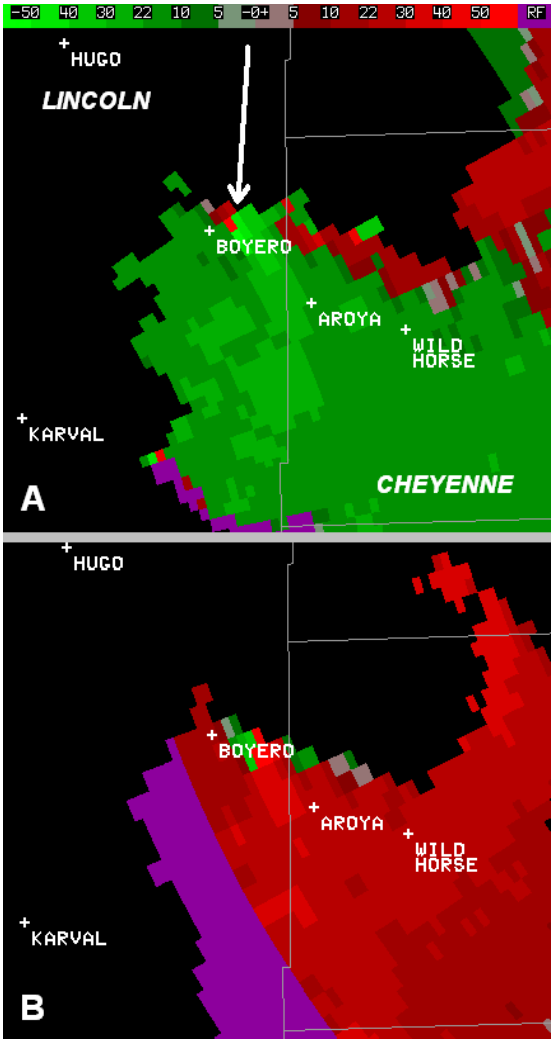

Figure 5. 0.5° elevation angle SRM displays at 0034 UTC, 16 June 2002, from Pueblo CO (a) and Goodland KS (b). County names, arrow toward mesoanticyclone and velocity scale are provided in (a). Locality names appear on both images, which are scaled identically. PUX and GLD radars were located generally SW of (a) and NE of (b) respectively.

---

100 kt (40-50 m s^{-1}) peak azimuthal shears were evident at each five minute interval through 0100, as the storm passed over Aroya and began to turn southeast. This represents at least 45 minutes duration of $\geq$80 kt (40 m s^{-1}) anticyclonic shear associated with this supercell's circulation.

The lead author intercepted and photographed the supercell during this peak phase (i.e., Fig. 6). Relatively hard, smoothly surfaced, spherical hail up to 2 inches (5 cm) in diameter was observed in the forward (southeast) precipitation flank, which damaged his vehicle and which was reported to the responsible NWS warning offices at Boulder, CO, and Goodland, KS. There also was distinct visual evidence of low level clockwise rotation in the relatively precipitation-free updraft region of the storm as the mesoanticyclone approached and passed immediately north through east of a stationary viewing position 1.6 km SW of Aroya. Hailstones began to fall beneath the updraft region at about 0100, while continuing from both the forward flank (east) and the rear-flank (west) downdrafts on either side of the mesoanticyclone. The hail remained roughly constant in distribution, maximum size and texture throughout the storm-relative (but stationary in ground speed) transect; however, accompanying rainfall diminished markedly from forward flank through the south rim of the mesoanticyclone. Precipitation remained largely hail from there into the rear flank, accompanied by intermittent light rain and drizzle. The hail accumulated to a depth of up to 10 cm over several mi^2 of short-grass range land southwest of Aroya.

As more hail was observed around the updraft base, the storm turned and accelerated east-southeastward, moving from 280° at 34 kt (17 m s^{-1}).

Figure 6. Scanned 35 mm transparency photograph (top) of the anticyclonic supercell, looking NW from 1.6 km SW of Aroya, CO at ~0025Z, 16 Jun 2002. Its mirror image (center) would look SW if also mirroring the direction of view relative to storm motion. The bottom image, for comparison, is from a 35 mm transparency of a tornadic, cyclonic supercell (~10 min after one tornado and 2 min before the next), 4 October 1998, looking SW from 6.4 km WSW of Dover, OK. Photos provided by the lead author.

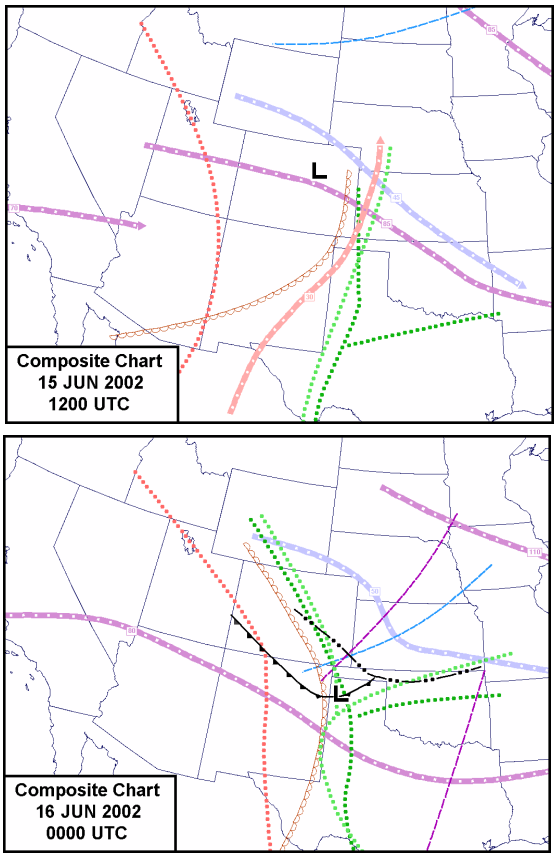

Figure 7. Composite charts as labeled. Thick purple (blue) lines denote 250 mb (500 mb) jets maxima. Thin purple (blue) lines are 250 (500) mb height troughs. Dotted green lines represent moist axes at 700 and 805 mb respectively. Scalloped brown line collectively represents the 700 and 805 mb drylines, which were practically juxtaposed at each analysis time. Dotted red line is the 805 mb thermal axis. Surface features (low, cold front, outflow boundary) are conventionally drawn except in black.

During this fourth motion phase – still left of the mean wind – the storm weakened, as evident visually and in reflectivity and SRM trends (not shown), and it dissipated by about 0130 in southern Cheyenne County.

3. ENVIRONMENTAL OVERVIEW

Subjective upper air analyses were performed at 250, 500, 700 and 805 mb pressure levels for full suite of synoptic rawinsonde data at 15/1200 and 16/0000. Also examined were special soundings launched at 1500, 1800 and 2100, in support of the International H20 Project (IHOP). [The 805 mb level was used instead of the more common 850 mb operational standard, because of the latter being underground across much of the area. Given the ground elevation of 1500-2000 m in this area, the 805 and 700 mb levels may serve as a proxy for the roughly equivalent 925 and 850 mb levels over the low plains farther east.] These data were blended with hourly plots of profiler winds, WSR-88D velocity azimuth display wind profiles (VWP) and surface observations for composite analyses. Results are summarized graphically in Fig. 7.

The area was under a general northwest flow regime aloft, characterized at 1200 by a roughly 70-90 kt (35-45 m s^{-1}) 250 mb jet and a weak 500 mb trough located well to the north from northern Minnesota to Montana. By 1800, regional profiler winds and the intermediate sounding at Denver (not shown) indicated this trough had reached extreme north-central Colorado, south-central Wyoming and western Nebraska. By 0000 on the 16th that trough had moved to southeastern Nebraska, central Kansas and extreme southeastern Colorado. This trough's proximity to eastern Colorado was timed with peak insolation-related heating of the air mass along and behind a surface cold front. This appeared to contribute to steepened lapse rates, based on modified RUC soundings and time series comparisons of 1200, 1800 and 0000 balloon soundings. The low level dryline had retreated across Colorado through the day, a process aided by weak moist advection behind the front in the boundary layer.

At the surface, only broad, weak baroclinicity was evident across the central high plains at 1200, with a weak surface low near Limon. By 1500, a surface low was analyzed over Akron, Colorado, with a weak cold front developing southwestward to near Limon, then westward to near Monument. By 1800, the frontal low had become ill-defined, and another had formed near Pueblo at a surface thermal maximum. The cold front then was crossing a broad, zonally oriented, topographic ridge near Limon known as the Palmer Divide, as well as the I-70 corridor near the Kansas border. The front continued southward through the Arkansas River valley of southeastern Colorado around 2100, then by 0000 on the 16th, into northeastern New Mexico (Fig. 7).

Thunderstorms developed along and behind the surface cold front (i.e., Fig. 1) throughout the day, beginning as early as 1500 to the south of Akron, and around 1800 along the Palmer Divide. Associated cloud and precipitation coverage became more widespread from the Palmer Divide southward and southeastward through the afternoon, as observed visually from the ground and on radar and satellite imagery. The aggregate outflows modified the surface air to be substantially colder than the ambient postfrontal air mass. By 2100, temperatures immediately behind the front in southeastern Colorado remained in the 82-86^{O} F (28-30^{O}C) range, while post-frontal outflow temperatures were falling generally into the 75-78^{O}F (24-26^{O}C) range. By 0000 the difference was even more pronounced, with outflow air as cold as 66^{O}F (19^{O}C) over easternmost

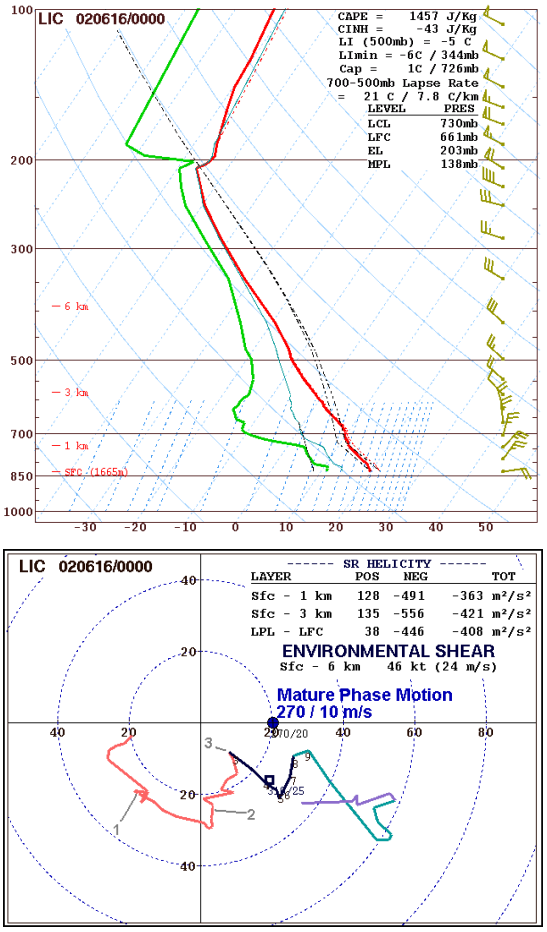

Figure 8. RUC model initial sounding for Limon, CO (LIC), 00 UTC, 16 Jun 2002, plotted as a *Skew-t* diagram (top) and hodograph (bottom) with annotated parameter values on each. Wind barbs (flags) represent 5 (25) m s^{-1} speeds. On the hodograph, isotachs are labeled in kt but with mature phase storm speed noted at 10 m s^{-1}; and heights from 1 to 3 km are labeled in bold gray.

Colorado near Burlington, and post-frontal temperatures 84-90^{O}f (29-32^{O}C) near the southeast corner of Colorado.

The Aroya supercell developed well north of the surface cold front and outflow boundary, along the northwest periphery of a large complex of thunderstorms that covered much of southeastern Colorado (evident in visible imagery, Fig. 1). No boundaries were evident either in surface analyses, reflectivity or satellite data at the genesis location, which was along the Palmer Divide. Differential heating and associated solenoidal ascent along the edge of the large anvil canopy may have contributed to this storm's origin in a weakly capped environment, based on a lifted RUC surface parcel (Fig. 8a); but observational data coverage is insufficient to verify such a process.

Hourly RUC soundings have been shown to reliably represent the environments of discrete supercells (Thompson et al. 2003). Here, the 0000 RUC analysis point forecast sounding for Limon (Fig. 8a) closely approximated surface thermodynamic conditions observed both at Limon and in immediate vicinity of the storm. The RUC sounding was judged to be the most representative of conditions ambient to this storm, by comparison to the 15/1800 and 16/0000 Denver rawinsonde soundings, forecast soundings from the 1800 Eta model, and initialized 0000 Eta soundings (not shown).

Our initial hypothesis was that this storm was elevated atop cold air from the north side of the front that had been further reinforced by outflows. However, further examination indicates that the storm probably was surface based, despite the postfrontal and postconvective environment characterized by "cool" 68-70^{O}F (20-21^{O}C) inflow air temperatures (as measured by the lead author and observed at Limon, 40 mi (65 km) to the northwest. Surface-based CAPE using the virtual temperature correction (Doswell and Rasmussen 1994) is estimated to be nearly 1500 J kg^{-1} based on the RUC sounding, amidst roughly 8^{O}C km^{-1} midtropospheric lapse rates.

During its anticyclonic rotation phase, the supercell moved leftward of both the mean wind and mean shear vectors and the hodographs through 0-1 and 0-3 km above ground level (AGL). This is consistent with negative values of storm-relative helicity (SRH) expected and commonly documented for surface-based left-movers (i.e., Bunkers 2002, Edwards et al. 2004). However, the 0-1 and 0-3 km AGL SRH for this case – given any of the four dominant motion vectors in its lifespan -- was considerably larger in magnitude and more negative than averages or medians for the Bunkers (2002) or Edwards et al. (2004) left-moving supercells. During the mature, eastward-moving phase near Aroya, the RUC hodograph with input observed storm motion yielded 0-1 km (0-3 km) net SRH of -363 m^2s^{-2} (-421 m^2s^{-2}). Among favorable Galilean-invariant parameters for supercells was 24 m s^{-1} shear through the 0-6 km AGL layer, and 59 m^2s^{-2} bulk Richardson number shear (each after Weisman and Klemp 1982).

4. VISUAL CHARACTERISTICS

Cloud and precipitation debris from other convection (evident east of the Aroya storm in Figs. 1 and 2) obscured the view of the supercell upon ground level approach from the Lamar area to the southeast. As the storm came into view from near Aroya, it exhibited classical supercell structures with a rain-free base, striated low-middle level cloud decks and pronounced forward-flank precipitation core.

To better aid conceptualization of this structure for storm observers, the photograph of this storm near peak intensity, showing these structures, is flipped into mirror image in Fig. 6. Given the storm's overall motion toward the east-southeast, a mirror for the

spotting angle would be for a storm moving toward the east-northeast.

Although this storm was nontornadic, the mirror image of its cloud features bore striking structural resemblance to a cyclonic, tornadic supercell on 4 October 1998 near Dover, OK, as also evident in Fig. 6. The Dover storm was within a few minutes of producing a tornado from the lowest cloud base at left, which was beginning to rotate strongly at the time of the photo. By contrast, only weak cloud-base rotation was evident in the Aroya storm from the time of the photograph until it passed overhead (at the same vantage point); and a tornado never appeared imminent. The intense shears detected in middle levels of the storm, as shown in Fig. 5, were not visually evident lower in the storm and at cloud base.

5. SUMMARY AND DISCUSSION

This case illustrates that environments behind both cold fronts and reinforcing convective outflows still may support supercells with significant severe weather, i.e., the 2 inch (5 cm) hail occurring here.

The ambient vertical wind profile was typical for a cold advection regime in that it that backed with height, which also is an ideal wind profile for large negative SRH given an embedded, left-moving storm. Left-movers are likely not as common as right-moving supercells because of this association with cold advection and the detrimental effect that such cooling can have on buoyancy. However, this event illustrates that, to the extent that the RUC sounding was representative of the environment, surface-based CAPE was more than adequate to support left-moving supercells, despite the presence of post-frontal, post-convective cold air advection in the boundary layer. Adjusting for the context of left-movers, this reinforces the concept of favorable surface-based buoyancy on the “cold” side of baroclinic boundaries (i.e., VORTEX findings of Markowski et al. 1998) – whether storms cross such a boundary or, as in this event, initiate well behind it.

One important question that may be unanswerable for this case, given 1) its surface-based nature, and 2) its long-lived, intense mesoanticyclone is: Why did this storm not produce a tornado? Tornadic left-movers have been documented (i.e., Monteverdi et al. 2001, Dostalek et al. 2004) in environments with only 500 J kg^{-1} more CAPE and weaker SRH. More detailed and dense field observations such as those performed in field experiments such as VORTEX might contribute to better understanding of the difference between tornadic and nontornadic processes in left-movers as well.

IHOP intermediate soundings, in combination with profiler and VWP data and hourly RUC soundings, were useful in assessing the thermodynamic and kinematic evolution of features above the surface throughout the day, in between synoptic balloon launches. Intermediate rawinsonde launches often are requested regionally by SPC forecasters on days of exceptional concern; and this case emphasizes the benefit both asynoptic observed soundings and RUC hourly model soundings. This study also underscores the need for subjective analysis and detailed utilization of multiple platforms therein. The subtle and still poorly understood character of initiation foci for convection north of the cold front supports the need for more dense surface data of the sort provided by the Oklahoma Mesonet (Brock et al. 1995), benefitting both post-mortem research and real-time operational forecasting of mesoβ- and smaller-scale convective processes.

This event illustrates that the anticyclonic supercell, when observable in the field, may be treated as a visual and conceptual mirror image of the cyclonic supercell for application to spotter training and for understanding their structure and morphology.

Finally, storm observation in the field remains an immeasurably valuable tool in assessment and verification of severe weather events. Several spotters and storm chasers contributed severe weather information, both in real time and *post facto*, to the concerned NWS warning offices in Boulder, CO, and at Goodland, KS. Without their presence in this event and in others in the Great Plains every spring, neither precise and accurate warning verification nor field documentation such as that herein would be as common. Furthermore, resulting documentation – including still photography and video – is commonly used for subsequent spotter training. A responsible and well-trained fleet of spotters and mobile storm chasers has been demonstrated in many instances (i.e, Pietrycha and Fox 2004) to benefit both real-time warning operations and subsequent research, and should be encouraged and supported wherever possible.

6. ACKNOWLEDGMENTS

The authors thank Paul Wolyn of NWS Pueblo, along with NWS Central Region and the SPC Scientific Support Branch, for generously supplying data and platforms for analysis both at Pueblo and Norman. Thanks to Elke (Ueblacker) Edwards for her intercept navigation and to Al Pietrycha for his skilled nowcasting, both of which made close observation and documentation of this storm possible from afield. Steve Weiss (SPC) provided very helpful encouragement, guidance and internal review.

7. REFERENCES

Brock, F.V., K. C. Crawford, R.L. Elliott, G.W. Cuperus, S.J. Stadler, H.L. Johnson, and M.D. Eilts, 1995: The Oklahoma Mesonet: A technical overview. *J. Atmos. Oceanic Technol.*, **12**, 5-19.

Bunkers, M.J., 2002: Vertical wind shear associated with left-moving supercells. *Wea. Forecasting*, **17**, 845-855.

Davies-Jones, R.P., 1986: Tornado dynamics. *Thunderstorm Morphology and Dynamics*. 2nd Ed., E. Kessler Ed., University of Oklahoma Press, 197-236.

Dostalek, J.F., J.F. Weaver and G.L. Phillips, 2004: Aspects of a tornadic left-moving thunderstorm on 25 May 1999. *Wea. Forecasting*, **19**, 614-626.

Doswell, C.A., III, and E.N. Rasmussen, 1994: The effect of neglecting the virtual temperature correction on CAPE calculations. *Wea. Forecasting*, **9**, 625-629.

Edwards, R., R.L. Thompson and C.M. Mead, 2004: Assessment of anticyclonic supercell environments using close proximity soundings from the RUC model. Preprints, *22nd Conf. on Severe Local Storms*, Hyannis, MA, Amer. Meteor. Soc. (this volume).

Klemp, J.B., and R.B. Wilhelmson, 1978: Simulations of right and left moving storms produced through storm splitting. *J. Atmos. Sci.*, **35**, 1097-1110.

Lemon, L.R., and C.A. Doswell III, 1979: Severe thunderstorm evolution and mesocyclone structure as related to tornadogenesis. *Mon. Wea. Rev.*, **107**, 1184-1197.

Markowski, P.M., E.N. Rasmussen, J.M. Straka, 1998: The occurrence of tornadoes in supercells interacting with boundaries during VORTEX-95. *Wea. Forecasting*, **13**, 852-859.

Mathews, G.N., and T.J. Turnage, 2000: An example of a left-split supercell producing 5-inch hail: The Big Spring, Texas storm of 10 May 1996. Preprints, *20th Conf. on Severe Local Storms*, Orlando, FL, Amer. Meteor. Soc., 526-529.

Monteverdi, J.P., W. Blier, G.J. Stumpf, W. Pi, and K. Anderson, 2001: First WSR-88D documentation of an anticyclonic supercell with anticyclonic tornadoes: The Sunnyvale-Los Altos, California, tornadoes of 4 May 1998. *Mon. Wea. Rev.*, **129**, 2805-2814.

Neilsen-Gammon, J.W., and W.L. Read, 1995: Detection and interpretation of left-moving severe thunderstorms using the WSR-88D: A case study. *Wea. Forecasting*, **10**, 127-140.

Pietrycha, A.E., and M. Fox, 2004: Effective use of various communication methods during a severe convective outbreak. Accepted to *Nat. Wea. Digest*. Available online at: http://www.stormeyes.org/pietrycha/030515/nwawebversion.pdf

Thompson, R.L., R. Edwards, J.A. Hart, K.L. Elmore and P.M. Markowski, 2003: Close proximity soundings within supercell environments obtained from the Rapid Update Cycle. *Wea. Forecasting*, **18**, 1243-1261.

Weisman, M.L., and J.B. Klemp, 1982: The dependence of numerically simulated convective storms on vertical wind shear and buoyancy. *Mon. Wea. Rev.*, **110**, 504-520.